European Congress on Computational Methods in Applied Sciences and Engineering
ECCOMAS 2004
P. Neittaanmäki, T. Rossi, K. Majava, and O. Pironneau (eds.)
V. Capasso and W. Jäger (assoc. eds.)
Jyväskylä, 24–28 July 2004

NUMERICAL INVESTIGATION OF SURFACE RUNOFF IN HILLSLOPES WITH VARIABLY SATURATED FLOWS

H. Beaugendre*, A. Ern*, T. Esclaffer† and E. Gaume†

*ENPC, Cermics,
6 et 8 avenue Blaise Pascal, cité Descartes, 77455 Marne-la-Vallée, France
e-mails: beaugend@cermics.enpc.fr, ern@cermics.enpc.fr

† ENPC, Cereve,
6 et 8 avenue Blaise Pascal, cité Descartes, 77455 Marne-la-Vallée, France
e-mails: esclaffer@cereve.enpc.fr, gaume@cereve.enpc.fr

Key words: Dynamics of watertables, Surface runoff, Dynamics of hillslopes, Numerical solutions.

Abstract. *During heavy rainfall episodes, subsurface flow can saturate the soil in various regions near the surface and, therefore, contribute to the production of overland flow. This paper investigates numerically watertable dynamics in partially saturated porous media and the coupling mechanisms between the hydraulic state of the soil and the genesis of surface runoff. Variably saturated flows are modeled using Richards' equation discretized using a finite element method (P_1-conforming) on unstructured, non-uniform triangulations. Two strategies are considered to model the coupling between the subsurface water table and surface runoff. The first strategy neglects the height of the overland flow as well as re-infiltration processes. The water table position being an unknown of the problem, its intersection with the ground surface yields an unsteady obstacle-type problem. A more detailed approach consists of modeling the overland flow using a simplified form of the Saint-Venant equations, yielding the so-called diffusive wave approximation. Numerical results are presented to compare both approaches.*

1 INTRODUCTION

The mechanisms leading to surface runoff on hillslopes exposed to heavy rainfall episodes have received significant attention over the last decades. Historically, the first approach considers streamflow to be generated by runoff over areally extensive portions of a watershed, where rainfall intensity overcomes soil infiltration capacity (Horton [1], 1933). This concept has been improved by the introduction of the partial area contribution approach initiated by Cappus [2] (1960) and Betson [3] (1964) whose work has been further developed by Dunne and Black [4] (1970). In this approach, the actual surface contributing to streamflow is restricted to saturated surfaces (where the water table reaches the surface level). Thus, the contributing area might represent only a small portion of the watershed, and its extension may vary in time and space. These studies lead to a segmentation of the watershed into infiltration, runoff and exfiltration dominated zones. An important issue is to determine the relative importance of surface and subsurface water in storm hydrographs. Several field and laboratory studies have been conducted (Abdul and Gillham [5], Barros *et al.* [6]) and revealed that field results are strongly site-dependent, whereas laboratory tests are complex and time-consuming. The need for numerical experiments to achieve faster results and more flexibility has rapidly raised (Ogden and Watts[7], Weiler and McDonnell [8]).

A widely used model to simulate partially saturated flow in porous media is the solution of Richards' equation. The complexity of this problem lies in the non-linearity of the equation resulting from the pressure-head-saturation relation and the non-linearity caused by the changing character of the boundary conditions owing to the movement of the water table. These difficulties have been challenged by a great number of researchers who have explored many ways: choice of the main unknown (Celia *et al.*, 1990 [9]), of a non-linear iterative solver, and of the space and time discretization scheme. Recently, this type of model has been used to investigate the mechanisms leading to surface runoff in hillslopes (Ogden and Watts [7], Cloke *et al.* [10]). These studies have emphasized the need for an accurate description of soil hydraulic parameters.

In the proposed approach, the pressure head h is chosen as the main unknown of the problem. Richards' equation is discretized using a finite element method (P^1 conforming) on unstructured, non-uniform triangulations $\mathcal{T}_h$. Two strategies are considered to model the coupling between the subsurface and the surface motion of the water. The first strategy neglects the height of the overland flow as well as re-infiltration processes and simply imposes a head boundary condition downstream of the intersection point. The water table position being an unknown of the problem, its intersection with the ground surface is treated as an unsteady obstacle-type problem. A more detailed approach consists in modeling the overland flow with a simplified form of the Saint-Venant equations, yielding the so-called diffusive wave approximation. The behavior of the fluid in the two regions is described by different partial differential equations. To close the problem, suitable interface conditions relating the unknowns from the two sub-domains across the interface

are needed. These two approaches are compared on two geometries, the first one at the metric scale and the second one at the hectometric scale. These test cases are also used to investigate the impact of hydraulic properties, boundary conditions, and initial condition on saturated area prediction.

2 GOVERNING EQUATIONS

The soil is modeled as an isotropic variably saturated porous medium, in which the movement of liquid water can be described by Richards' equation

$$\partial_t \theta(h) = \partial_x \cdot \Big(k(h) \cdot \partial_x \varphi \Big) , \tag{1}$$

where t is the time (T), x is the space coordinate (L), θ is the volumetric water content (dimensionless), k the unsaturated hydraulic conductivity (LT^{-1}), h the soil water pressure head (L), and $\varphi = h + z$ the total hydraulic head (L) where z is the vertical coordinate (upwards). In particular, the use of Richards' equation assumes that there is no air pocket trapped by the flow. The Darcy flow velocity (LT^{-1}) is defined by

$$v(h) = -k(h) \cdot \partial_x \varphi = -k(h) \cdot \partial_x h - k(h) \cdot e_z \, , \tag{2}$$

with e_z the upward unit vector.
Eq.(1) requires knowledge of the soil water retention curve, $\theta(h)$, and the unsaturated hydraulic conductivity function, $k(h)$. Many empirical equations have been used to describe the relations between water content, pressure and hydraulic conductivity (Brooks and Corey [11], Mualem [12], van Genuchten [13]). The choice of one of these models strongly conditions the hillslope hydrology [10], especially near saturation and therefore influences the position of the water table. In this paper hydraulic conductivity and water content will be described using the van Genuchten model (VGM model). Let $n > 1$ and α be the van Genuchten soil parameters, and set $m = 1 - 1/n$. The van Genuchten model (VGM model) [13] is

$$\widetilde{\theta}(h) = \begin{cases} \left(1 + (-\alpha h)^n\right)^{-m} \, , & h < 0 \, , \\ 1 \, , & h \geq 0 \, , \end{cases} \tag{3}$$

where $\widetilde{\theta}(h) = \frac{\theta(h) - \theta_r}{\theta_s - \theta_r}$ is the effective saturation, θ_r and θ_s being the residual and saturated water content, respectively. Letting k_s be the saturated hydraulic conductivity, we set $k(h) = k_s k_r(h)$ where the relative hydraulic conductivity is specified as a function of $\widetilde{\theta}(h)$:

$$k_r(\widetilde{\theta}) = \begin{cases} \widetilde{\theta}^{1/2} \left[1 - \left(1 - \left(\widetilde{\theta} \right)^{1/m} \right)^m \right]^2 \, , & h < 0 \, , \\ 1 \, , & h \geq 0 \, . \end{cases} \tag{4}$$

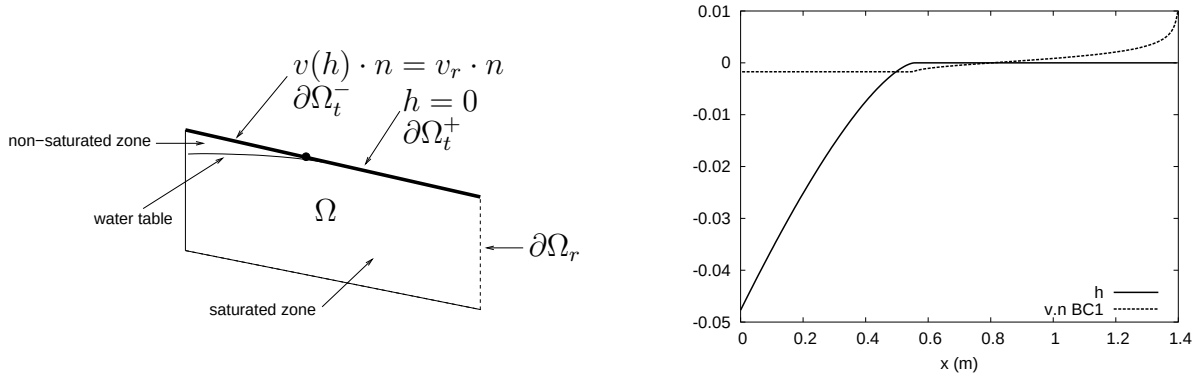

Figure 1: Left: schematic representation of the domain Ω. Right: typical pressure head, h (m), and normal velocity, $v \cdot n$ (m/h), distribution along the top surface, at saturation $h = 0$.

3 OBSTACLE-TYPE MODEL (OTM code)

In this model, the feedback of surface runoff on the water table dynamics is neglected. The height of the overland flow as well as re-infiltration processes are neglected and we simply impose a head boundary condition downstream of the intersection point. Consider the two-dimensional domain Ω (its boundary $\partial\Omega$) sketched on the left panel of figure 1. Let n be the normal vector outwards to the surface. A constant rainfall intensity i (LT^{-1}) is considered; the rainflow velocity is defined as $v_r = -i\, e_z$ where e_z is the upward unit vector so that $i \geq 0$. The upper surface of the model domain (top boundary: $\partial\Omega_t$) allows infiltration and exfiltration. The top boundary may be divided into two regions

- $\partial\Omega_t^-$ the non-saturated region: $h \leq 0$ and $v \cdot n = v_r \cdot n$
- $\partial\Omega_t^+$ the saturated region: $h = 0$ and $v \cdot n \geq v_r \cdot n$

The saturated region may also be divided into two subregions, see right panel of figure 1:

- the saturated zone that still allows some infiltration: $h = 0$ and $v_r \cdot n \leq v \cdot n \leq 0$
- the exfiltration region: $h = 0$ and $v \cdot n > 0$.

For the bottom and left boundaries we assume an impermeable layer, i.e. we impose $v \cdot n = 0$. On the right boundary $\partial\Omega_r$, two kinds of boundary conditions are considered in this paper:

- BC1: no-flow boundary condition at the right surface (representing an impermeable condition or a symmetry condition);
- BC2: constant total hydraulic head, φ, at the right surface (accounting for the presence of a stream).

3.1 Steady problem

One can prove that a steady-state solution exists whenever $i \leq k_s$. For the sake of simplicity we present the algorithm assuming a BC1 boundary condition on $\partial\Omega_r$. Recall that H^1 is the space of square integrable functions whose distributional derivative is also square integrable. The weak formulation corresponding to the steady problem is the following: given $\partial\Omega_t^+ \subset \partial\Omega_t$, let

$$V_{\partial\Omega_t^+} = \left\{ \phi \in H^1(\Omega);\ \phi = 0 \text{ on } \partial\Omega_t^+ \right\}, \tag{5}$$

and let a be the form (non-linear in h, linear in ϕ):

$$a_{\partial\Omega_t^+}(h,\phi) = \int_\Omega k(h) \cdot (\partial_x h + e_z) \cdot \partial_x \phi + \int_{\partial\Omega_t^-} (v_r \cdot n)\, \phi\,. \tag{6}$$

Note that working with the space $V_{\partial\Omega_t^+}$ implies $h = 0$ on the saturated area $\partial\Omega_t^+$. Then, we seek $\partial\Omega_t^+ \subset \partial\Omega_t$ and $h \in V_{\partial\Omega_t^+}$ such that

$$\begin{cases} \text{(i)} & a_{\partial\Omega_t^+}(h,\phi) = 0 \quad \forall \phi \in V_{\partial\Omega_t^+}\,, \\ \text{(ii)} & h \leq 0 \quad \text{on } \partial\Omega_t^-\,, \\ \text{(iii)} & v(h) \cdot n \geq v_r \cdot n \quad \text{on } \partial\Omega_t^+\,. \end{cases} \tag{7}$$

Note that the well posedness of (i) requires that $\partial\Omega_t^+ \neq \emptyset$, i.e. that the water table has reached the top boundary. An approximate solution $\left\{\partial\Omega_t^+, h\right\}$ of (7) is sought using Newton's method embedded into a fixed-point iteration to determine those points lying on the soil surface where artesian conditions are met. The following iterative algorithm is proposed to solve the problem:

1. choose an initial $\partial\Omega_t^+$;
2. solve problem (i) using e.g. P^1 conforming finite elements;
3. check whether (ii) and (iii) are satisfied;
4. if (ii) is satisfied and (iii) is not, move $\partial\Omega_t^+$ one mesh cell (or more) down; go to step 2;
5. if (iii) is satisfied and (ii) is not, move $\partial\Omega_t^+$ one mesh cell (or more) up; go to step 2;
6. if both (ii) and (iii) are satisfied, then the current pair $\left\{\partial\Omega_t^+, h\right\}$ is the desired solution; one may refine the mesh and go back to step 2.

Owing to the maximum principle, both (ii) and (iii) can not be violated simultaneously. However, in numerical approximations, this may happen. In this case, we still consider that the water table has been correctly positioned. With this "loosened" convergence criterion, the final position of the water table depends from whether the converged position $\partial\Omega_t^+$ has been approached from below or above. The two resulting values give lower and upper bounds for the water table position (typically differing from one or two mesh cells at the most).

3.2 Unsteady problem

The unsteady problem is solved using an implicit Euler scheme. For a time step $k \geq 0$, given $(\partial\Omega_t^+)^k$ and h^k, we seek $(\partial\Omega_t^+)^{k+1} \subset \partial\Omega_t$ and $h^{k+1} \in V_{(\partial\Omega_t^+)^{k+1}}$ such that

$$\left\{\begin{array}{ll} \text{(i)} & \frac{1}{\delta t}\int_\Omega \big(\theta(h^{k+1}) - \theta(h^k)\big)\,\phi + a_{(\partial\Omega_t^+)^{k+1}}(h^{k+1},\phi) = 0 \quad \forall \phi \in V_{(\partial\Omega_t^+)^{k+1}}\,, \\ \text{(ii)} & h^{k+1} \leq 0 \quad \text{on } (\partial\Omega_t^-)^{k+1}\,, \\ \text{(iii)} & v(h^{k+1})\cdot n \geq v_r \cdot n \quad \text{on } (\partial\Omega_t^+)^{k+1}\,. \end{array}\right. \tag{8}$$

The problem is solved using the same iterative algorithm as in the steady problem. In step 1, the initial choice is $(\partial\Omega_t^+)^{k+1} = (\partial\Omega_t^+)^k$. Note that in the unsteady case, problem (i) is well-posed even if the water table has not reached the top boundary.

4 DIFFUSIVE WAVE MODEL (DWM code)

4.1 Governing equations

Transient flow of shallow water (both overland flow and open channel) can be described by the Saint-Venant equations,

$$\left\{\begin{array}{llllllll} \text{(i)} & \partial_t y & + & \partial_x(yV) & = & 0\,, & & \\ \text{(ii)} & \partial_t V & + & V\partial_x V & + & g\partial_x y & + & g(S_f - S) = 0\,, \\ & \text{(I)} & & \text{(II)} & & \text{(III)} & & \text{(IV)} \end{array}\right. \tag{9}$$

were y is the water depth (L), V is the flow velocity (LT^{-1}), g is the gravity (LT^{-2}), S is the river bed slope and S_f is the energy line slope (S and S_f are dimensionless).
We assume that in the momentum equation Eq.(9) (ii) terms (I) and (II) can be neglected in comparison with (III) and (IV). Thus we obtain the diffusive wave approximation which is widely used to describe flood routing:

$$\left\{\begin{array}{ll} \text{(i)} & \partial_t y + \partial_x(yV) = 0\,, \\ \text{(ii)} & \partial_x y + S_f - S = 0. \end{array}\right. \tag{10}$$

Basic assumptions underlying this model are [14, 15]:

- flow is one-dimensional (horizontal);

- pressure has hydrostatic distribution;
- distributed friction losses can be evaluated using the usual uniform flow formula [16].

The Manning-Strickler uniform flow formula is usually chosen to describe the energy line slope S_f [17, 18]:

$$V = K_S R^{2/3} S_f^{1/2}\,, \tag{11}$$

where K_S is the Strickler coefficient of roughness ($\mathrm{L}^{-1/3}\mathrm{T}^{-1}$) and R the hydraulic radius (L) defined as the ratio between the cross sectional flow area A (L^2) and the wet perimeter χ (L).
Assuming that overland flow occurs as a thin layer with a wide rectangular section of width B, the relation $y \ll B$ is granted. Hence, $A = By$, $\chi = B + 2y$ and

$$R = \frac{B.y}{B + 2y} \approx y\,. \tag{12}$$

Let $q(y) = yV$, using Eq.(10) (ii) and Eq.(12) in Eq.(11) yields

$$q(y) = K_S.y^{5/3}.\sqrt{(\partial_x y + S)}\,. \tag{13}$$

The continuity equation then becomes:

$$\partial_t y + \partial_x q(y) = 0. \tag{14}$$

4.2 Coupling method

Considering the hydrostatic distribution of pressure in shallow water, we assume the following relation between the variable y describing the surface flow and the variable h describing the subsurface flow:

$$y = \begin{cases} h\,, & \text{on } \partial\Omega_t^+, \\ 0\,, & \text{on } \partial\Omega_t^-\,. \end{cases} \tag{15}$$

Taking into account the mass transfer from the subsurface flow into the surface flow yields the continuity equation

$$\partial_t h + \partial_x q(h) = v(h) \cdot n \quad \text{on} \quad \partial\Omega_t^+\,. \tag{16}$$

A finite element/finite volume method is used for the discretization in space: a finite element method is used for Richards' equation and a finite volume method is used for the diffusive wave equation.

Let $P_c^1(\mathcal{T}_h) = \left\{ v_h \in \mathcal{C}^0(\overline{\Omega}) / \forall T \in \mathcal{T}_h \, , v_{h|T} \in P^1(T) \right\}$ where $P^1(T)$ is the space of polynomials on T with degree ≤ 1. We consider the discrete problem

$$\frac{1}{\delta t} \int_\Omega \left(\theta(h^{k+1}) - \theta(h^k) \right) \phi + a_{(\partial\Omega_t^+)^{k+1}}(h^{k+1}, \phi) = R(h^k, h^{k+1}, \phi) \quad \forall \phi \in P_c^1(\mathcal{T}_h) \tag{17}$$

where

$$R(h^k, h^{k+1}, \phi) = - \int_{\partial\Omega_t^+} \left(\frac{h^{k+1} - h^k}{\delta t} \phi + \partial_x q(h^{k+1}) \phi \right) . \tag{18}$$

In the current DWM implementation the hydraulic conductivity in $a_{(\partial\Omega_t^+)^{k+1}}$ is defined explicitly in time.

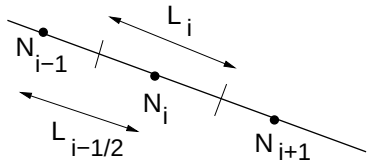

Figure 2: Details of the space discretization at the soil surface.

A finite volume method is used to evaluate $R(h^k, h^{k+1}, \phi)$. The unsteady term is approximated with a mass lumping, i.e. for the vertex N_i located on $\partial\Omega_t^+$ (figure 2):

$$\int_{\partial\Omega_t^+} \left(\frac{h^{k+1} - h^k}{\delta t} \right) \phi \approx \frac{h_i^{k+1} - h_i^k}{\delta t} L_i \, . \tag{19}$$

The second term of $R(h^k, h^{k+1}, \phi)$ is approximated using an upwind scheme. We assume that the nodes on $\partial\Omega_t^+$ are numbered downwards defining the numerical flux $Q(h_{i-1}^{k+1}, h_i^{k+1}) = K_s (h_{i-1}^{k+1})^{5/3} \left(\frac{h_i^{k+1} - h_{i-1}^{k+1}}{L_{i-1/2}} + S \right)^{1/2}$, we set

$$\int_{\partial\Omega_t^+} \partial_x q(y) \phi \approx Q(h_i^{k+1}, h_{i+1}^{k+1}) - Q(h_{i-1}^{k+1}, h_i^{k+1}). \tag{20}$$

Eq.(20) is used for all nodes in the interior of $\partial\Omega_t^+$. At the outlet node, say N_{i_0}, we set $Q(h_{i_0}^{k+1}, h_{i_0+1}^{k+1}) = K_S h_{i_0}^{k+1} S^{1/2}$ which implicitly assumes $\partial_x h = 0$ at the outlet.
Regarding the BC2 boundary condition for the DWM, we assume that the nodes are numbered downwards on $\partial\Omega_r$. For two such nodes, say N_j and N_{j+1}, we impose

$$\forall (N_j, N_{j+1}) \in \partial\Omega_r \quad h_j + z_j = h_{j+1} + z_{j+1} \, . \tag{21}$$

Eq.(21) implies that the total hydraulic head $\varphi = h + z$ is spatially constant along $\partial\Omega_r$. At each time t, its value is $h_{i_0}(t) + z_{i_0}$, where z_{i_0} is the vertical coordinate of the node N_{i_0} at the toe of the slope and $h_{i_0}(t)$ is the corresponding pressure head.

5 NUMERICAL RESULTS

Simulations have been performed at the metric scale and at the hectometric scale. The metric-scale problem is used to investigate the effects of hydraulic properties and boundary conditions (BC1, BC2) on the dynamic response of the water table. For the hectometric-scale problem the effects of some geometrical properties, of the boundary conditions and of the initial condition are under study. Selected soil textures are summarized in table 1. Let L be the length of the slope, L_s be the portion of the hillslope that is saturated and $Q_{rain} = iL(e_z \cdot n)$ be the rainfall rate. We define Q_{in} to be the infiltration flux and $Q_{not\,in}$ the "direct runon" flux (the water that never infiltrates): $Q_{rain} = Q_{in} + Q_{not\,in}$. The exfiltration flux Q_{exf} corresponds to the top surface exfiltration $Q_{exf|\partial\Omega_t}$ plus the exfiltration into the stream $Q_{exf|\partial\Omega_r}$ (subsurface flow through the right surface) if any: $Q_{exf} = Q_{exf|\partial\Omega_t} + Q_{exf|\partial\Omega_r}$. Q_{runoff} is composed of the exfiltration and the "direct runon": $Q_{runoff} = Q_{exf} + Q_{not\,in} = Q_{exf} + Q_{rain} - Q_{in}$. The time to reach equilibrium Te is defined numerically as the lowest time for which $|Q_{in} - Q_{exf}| \leq 5 \times 10^{-3} Q_{in}$. At equilibrium $Q_{in} = Q_{exf}$ and, hence, $Q_{runoff} = Q_{rain}$. Note that Q_{runoff} is not the instantaneous water flux at the toe of the slope and into the stream but the instantaneous water flux into the overland flow and into the stream.

Texture	θ_r (-)	θ_s (-)	α (1/m)	n (-)	k_s (m/h)
Sand OW	0.069	0.435	0.326	3.9	5.0
Sand 1	0.045	0.430	14.5	2.68	0.297
Sand 2	0.05	0.5	3.7	5	0.1
YLC	0.23	0.55	3.6	1.9	0.018
SCL	0.1	0.41	1.9	1.31	0.0026

Table 1: VGM soil hydraulic parameters.

5.1 Metric-scale problem

The two-dimensional domain Ω (its boundary $\partial\Omega$) selected to perform the study is sketched in figure 3 and corresponds to the configuration considered by Abdul and Gillham [5]. The domain dimensions are 1.4 m in length and 1 m to 0.8 m in height. Two kinds of boundary conditions are considered on the right boundary: the BC1 and BC2 boundary conditions previously described. For the bottom and left boundaries we assume an impermeable layer. We impose $v \cdot n = 0$ at the upslope end (left boundary) and at the bottom surface of the domain. Simulations were run using a constant rainfall intensity, $i/k_s = 10\%$ (preventing Hortonian runoff), for a duration longer than the time necessary to reach equilibrium. The Strickler coefficient of roughness K_S is set to $10 m^{-1/3} s^{-1}$. We observed that when i/k_s is fixed, the ratio L_s/L at steady state is not affected by soil texture and depends only on geometrical and boundary considerations (figure 4). The shape

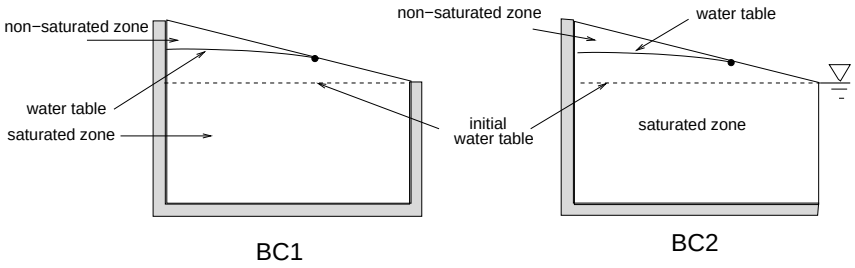

Figure 3: Abdul and Gillham geometry. Left: BC1 boundary condition. Right: BC2 boundary conditions.

of the three curves is a consequence of the respective shapes of the hydraulic functions for the three soils. More precisely, the value of the n parameter conditions the curvature of the plots. For instance, a sole modification of this parameter set to 5 for the YLC soil gives a similar response to that of the Sand 2 soil.

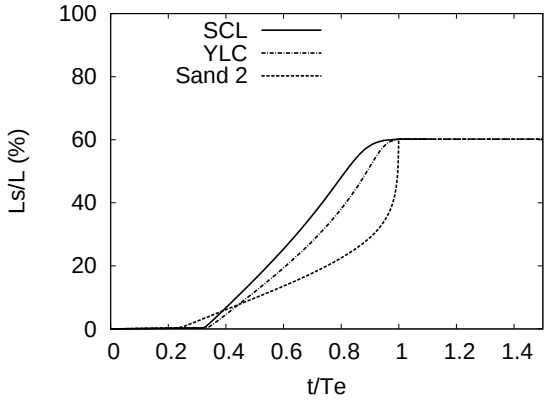

Figure 4: Temporal evolution of the relative hillslope saturated area for the three soils (SCL, YLC, Sand 2), $i/k_s = 10\%$, initial condition: horizontal water table at 0.7m, (OTM code, with BC1 boundary condition).

The evolution in time of the water table location has been studied for Sand 1 and YLC soils (table 1) using both boundary conditions, BC1 and BC2, and both modeling approaches. The initial condition is a horizontal water table located at 0.8 m (figure 3). Figure 5 displays the fraction of the hillslope saturated area, L_s/L, versus time t. These plots reveal the temporal response of the hillslope for both boundary conditions and both soils. The OTM and DWM codes give similar results. The time to achieve equilibrium is larger for the YLC soil than for the Sand 1 soil; this is related to the fact that k_s is the controlling parameter for the temporal response in this case. The final water table position is lower when a constant head boundary condition is imposed on the right surface compared to the no-flow boundary condition. This is related to the creation of a subsurface exfiltration on the right surface when BC2 is imposed. As a result of the water table position, the infiltration flux at steady state is higher for BC2 (figures 6 a and b).

At equilibrium, infiltration equals exfiltration and therefore exfiltration is higher for BC2. Note that the velocity vectors for the two boundary conditions are very different. By imposing BC2 boundary condition the velocity vectors on the saturated zone are nearly tangent to the surface: most of the exfiltration occurs through the right surface (into the stream). Figure 6 c shows the fraction of Q_{runoff} versus t for the two models and the two boundary conditions. At this space scale, the boundary condition clearly affects the dynamic evolution of Q_{runoff}. Similar results are observed for the YLC soil.

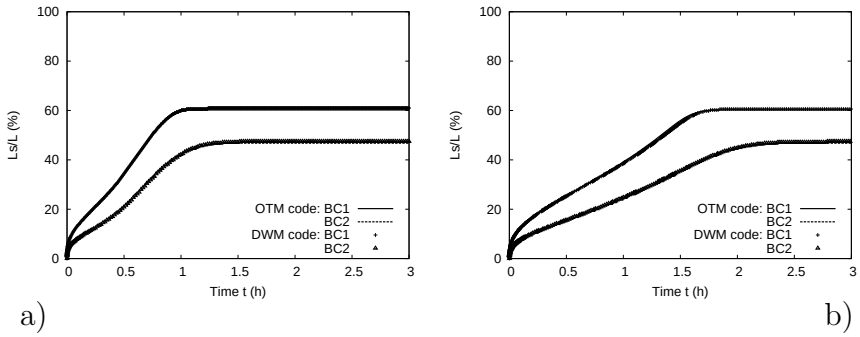

Figure 5: Model comparison of the dynamic evolution of the saturated area using BC1 or BC2 boundary condition for a) Sand 1 soil and b) YLC soil.

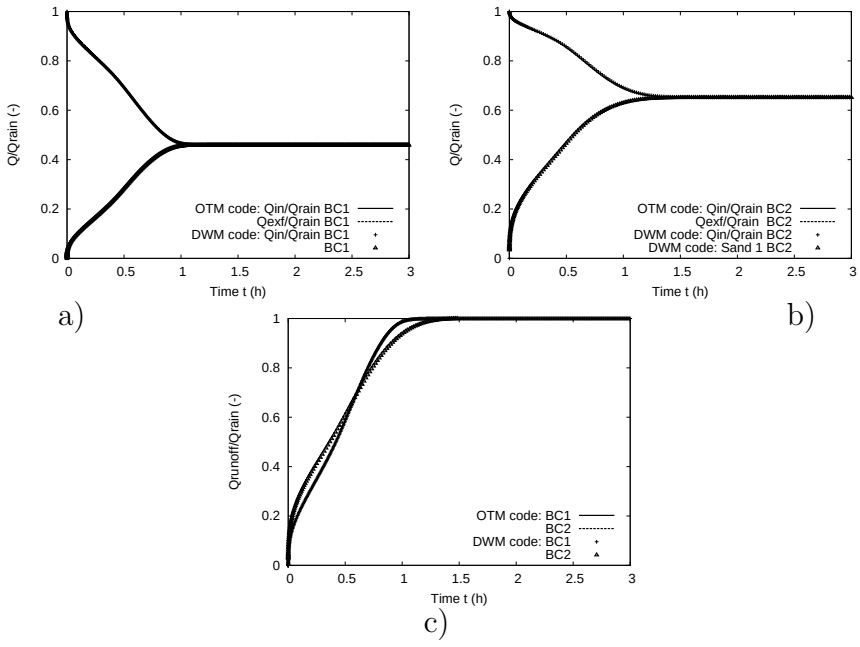

Figure 6: For Sand 1 soil: model comparison of the infiltration flux Q_{in}, the exfiltration flux Q_{exf} using a) BC1 boundary condition; b) BC2 boundary condition. c) Model comparison of Q_{runoff} for BC1 and BC2 boundary conditions.

5.2 Hectometric-scale model

The geometry [7] used in this case is presented in figure 7. A no-flow boundary condition is imposed at the bottom and left surfaces, simulating an impermeable layer. Simulations were run with a constant rainfall intensity, $i = 30mm/h$ ($i/k_s = 0.6\%$). The initial condition is a horizontal water table located at the toe of the slope (figure 7). The hillslope geometrical properties are the following: the slope angle So fixed and set to 10 %, the depth to impermeable layer D and the slope length L. The Sand OW proposed by Ogden & Watts (table 1) is the chosen soil for this geometry.

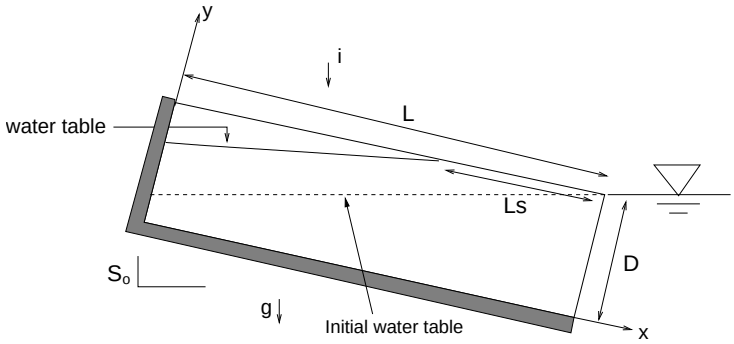

Figure 7: Ogden and Watts geometry.

5.2.1 Geometrical investigations

A constant head boundary condition is imposed at the right surface, representing a stream. Some geometrical properties (the slope length L and the depth D) are numerically investigated by the OTM code, using the BC2 boundary condition.

	$L = 30m$, $D = 1m$	$L = 50m$, $D = 1m$	$L = 50m$, $D = 2m$
Te (h)	1.43	5.98	11.97
$1 - \frac{Dk_sSo}{iL}$	44.4%	66.7%	33.3%
L_s/L	45.6%	67.3%	34.7%

Table 2: Equilibrium time, Te, using Sand OW soil and the three geometries. Comparison between the Ogden and Watts' analytical prediction for L_s/L and our numerical prediction.

Figure 8 shows the dynamic response of the hillslope for the following configurations: ($L = 50m$, $D = 1m$), ($L = 50m$, $D = 2m$) and ($L = 30m$, $D = 1m$). The relative hillslope saturated area agrees with Ogden and Watts' analytical considerations [7]: $\frac{Ls}{L} = 1 - \frac{Dk_sSo}{iL}$ (table 2). Ogden and Watts' analytical expression is based on the following assumption:

the hydraulic gradient is equal to the land surface slope So wherever the water table intersects the ground surface. At i, k_s, So and L fixed, the saturated area increases as D decreases (figure 8 a). At i, k_s, So and D fixed, the saturated area increases as L increases (figure 8 a). With BC2 imposed, the exfiltration flux occurs through the right surface and is proportional to D, indeed Q_{exf} is twice bigger when D is doubled, (figure 8 b). The time to reach equilibrium naturally increases with increasing soil depth and slope length (table 2).

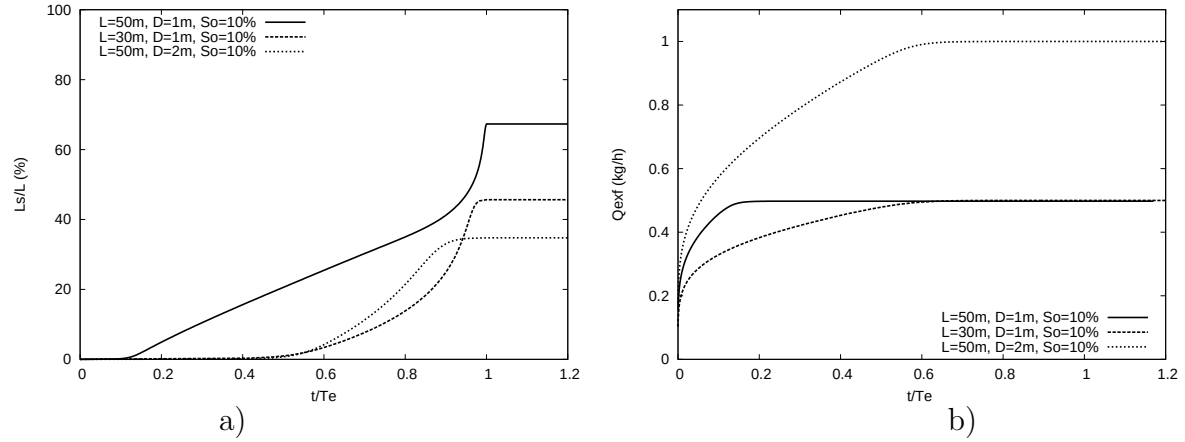

Figure 8: Using OTM code with BC2 boundary condition; a): Evolution in time of the relative saturated area for ($L = 50m$, $D = 1m$); ($L = 30m$, $D = 1m$) and ($L = 50m$, $D = 2m$); b): Exfiltration flux.

5.2.2 Boundary condition effects

Figure 9 shows the comparison between the two boundary conditions (BC1 and BC2) for the geometry $L = 50m$, $D = 1m$. At this space scale the impact of the boundary condition is negligible. The differences between the two solutions are localized at the toe of the slope (in the area near the stream) and change the nature of the exfiltration: top surface exfiltration for BC1 and subsurface exfiltration for BC2.

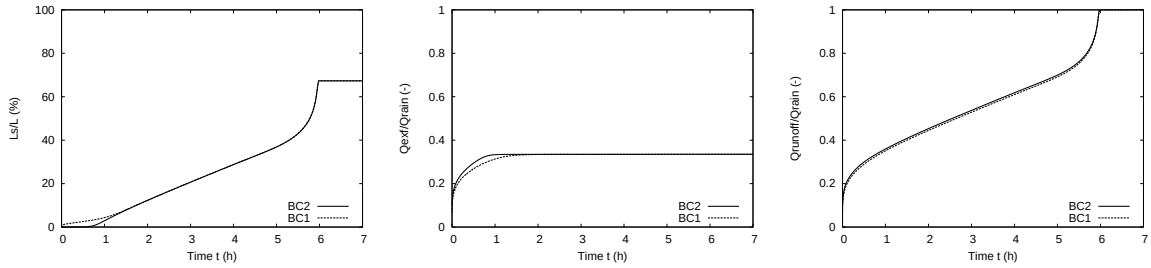

Figure 9: Investigation of the boundary condition effects on the evolution of the saturated area, Q_{exf} and Q_{runoff} (OTM code, geometry: $L = 50m$, $D = 1m$).

5.2.3 Model comparison

Figure 10 compares the results obtained with the two models on the geometry $L = 50m$, $D = 1m$, and $K_S = 10m^{-1/3}s^{-1}$. Both models give similar results, under these conditions. Neglecting the feedback of surface runoff on water table dynamics in this case seems to lead to reliable results. We notice a slight difference between the two models in the steady-state value of Q_{exf}, it is related to the way the head boundary condition, BC2, is imposed with the DWM.

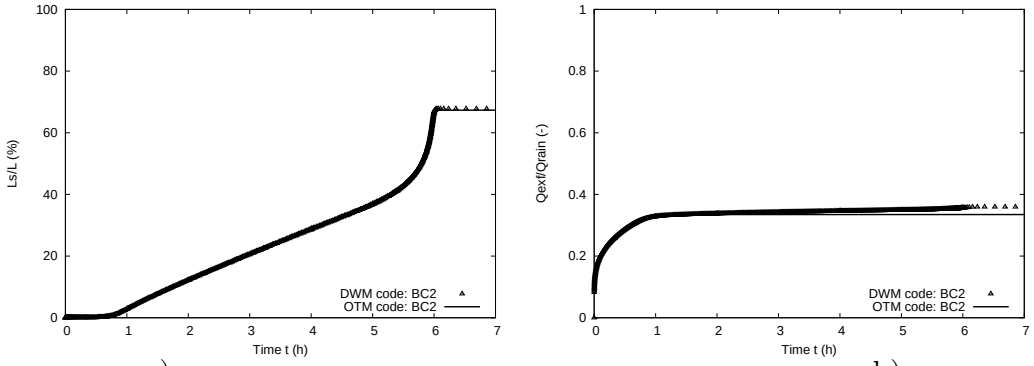

a) b)

Figure 10: Comparison of the two models for the BC2 boundary condition a) comparison of the evolution in time of the relative saturated area; b) comparison of the exfiltration flux.

Note

As can be seen in figure 11 a the texture of the soil selected for the hectometric-scale geometry is very specific. Its hydraulic conductivity decreases very slowly compared to YLC or Sand 1 soil. With this type of soil and the initial condition proposed by Ogden and Watts (horizontal water table at the toe of the slope) it is then possible to obtain a numerical solution with a reasonable mesh size (mesh spacing around 0.5 m and 1 m). The choice of an other soil, as YLC for example, will have required a much finer mesh. Indeed, the extremely low hydraulic conductivity of the soil on the left part of the geometry will induce a downward infiltration front. The choice of another initial condition, as proposed in figure 11 b, allows the computation of a solution. Figures 11 c and d show the evolution in time of the relative hillslope saturated area and the infiltration and exfiltration fluxes for the soil YLC with a rainfall intensity $i/k_s = 10\,\%$ and the geometry $L = 50m$, $D = 1m$. The ratio Q_{exf}/Q_{rain}, in this case is also in agreement with Ogden and Watts' analytical formula: $\frac{Q_{exf}}{Q_{rain}} = \frac{k_s SoD}{i(e_z \cdot n)L} \approx 0.02$.

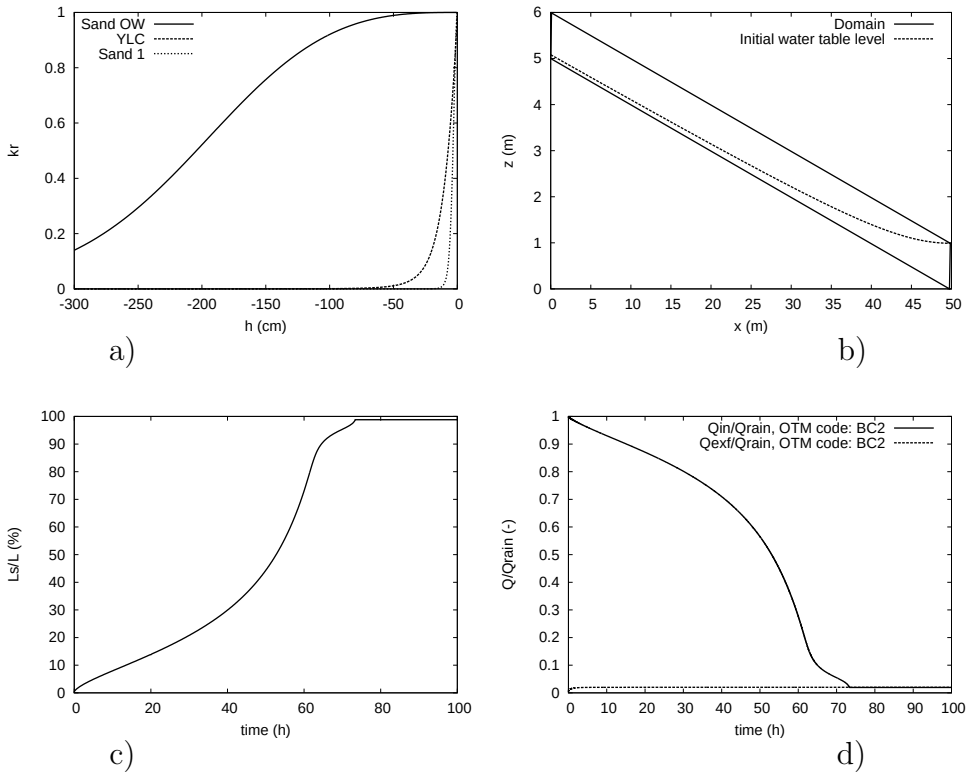

Figure 11: a) Relative hydraulic conductivity for Sand 1, YLC and Sand OW soils; b) YLC initial water table level; c) Evolution in time of the relative saturated area for YLC (OTM code, BC2 on the right surface); d) Evolution in time of the infiltration and exfiltration fluxes for YLC (OTM code, BC2 on the right surface).

6 CONCLUSION

Richards' equation combined with the van Genuchten's model for hydraulic functions has been discretized using finite elements in space. Two strategies are considered in order to model the coupling between the subsurface and the surface flow of the water. The first strategy (OTM code) neglects the height of overland flow as well as re-infiltration processes and simply imposes a head boundary condition downstream of the intersection point. The changing character of the surface boundary conditions owing to the movement of the water table yields an unsteady obstacle-type problem. A more detailed approach (DWM code) consists in modeling the overland flow with a simplified form of the Saint-Venant equations, yielding the so-called diffusive wave approximation. To close the problem, suitable interface conditions relating the unknowns from the two sub-domains across the interface are proposed. Both models have been used to investigate the hydraulic behavior of hillslopes under constant rainfall conditions.

Numerical results on the small-scale geometry have shown that for a fixed value of the ratio i/k_s, the texture of the soil, characterized by the van Genuchten hydraulic parameters, strongly affects the dynamic response of the system, whereas the steady-state values (L_s/L, Q_{in}, Q_{exf} and Q_{runoff}) remain identical. Because the range of k_s is wide for the soils presented in this study, a constant i/k_s ratio represents rainfall events strongly different (YLC: i = 1.8 mm/h, Sand 1: i = 29.7 mm/h). At the metric scale the ratio L_s/L is also strongly dependent on boundary conditions. On the Ogden and Watts geometry, the numerical results are in very good agreement with the analytical considerations of Ogden and Watts. At this space scale boundary conditions on the right surface have a marginal impact on the solution. This medium-scale problem also underlines the importance of the initial condition.

For both geometries presented in this paper, mechanisms leading to saturation are controlled by subsurface flows, i.e. the hydraulic properties of the soil. Modeling the overland flow in these cases does not lead to significant differences. The two models give similar results. Further comparisons involving re-infiltration processes will be conducted to investigate the impact of overland flow modeling on the genesis of surface runoff.

ACKNOWLEDGEMENTS

This work has been supported by INRIA under the Cooperative Research Project DYNAS (http://www-rocq.inria.fr/estime/DYNAS). We thank our colleagues from CEMAGREF and INRIA for stimulating discussions. We thank Patrick Dangla from LMSGC for providing the BIL code on which the DWM code has been implemented.

REFERENCES

[1] R.E. Horton, The role of infiltration in the hydrologic cycle, *Eos Trans. AGU*, **14**, 446–460, 1933.

[2] P. Cappus, Etude des lois de l'écoulement. Application au calcul et à la prévision de débits. Bassin expérimental de l'Alrance. La Houille Blanche A 493–520, July-August 1960.

[3] R.P. Betson, What is watershed runoff?, *J. Geophys. Res.*, No. **69(8)** 1541–1551, 1964.

[4] T. Dunne and R.D. Black, Partial area contributions to storm runoff in a small New England watershed, *Water Resour. Res.*, **6**, 1296–1311, 1970.

[5] A.S. Abdul and R.W. Gillham, Laboratory studies of the effects of the capillary fringe on streamflow generation, *Water Resour. Res.*, **20**, 691–708, 1984.

[6] A.P. Barros, D. Knapton, M.C. Wang and C.Y. Kuo, Runoff in shallow soils under laboratory conditions, *J. Hydraul. Eng.*, **4(1)**, 28–37, 1999.

[7] F.L. Ogden and B.A. Watts, Saturated area formation on non convergent hillslope topography with shallow soils : a numerical investigation, *Water Resour. Res.*, **36(7)**, 1795–1804, 2000.

[8] M. Weiler and J. McDonnell, Virtual experiments: a new approach for improving process conceptualization in hillslope hydrology, *J. of Hydrology*, **285**, 3–18, 2004.

[9] M.A. Celia, E.T. Boulotas and R.L. Zarba, A general mass-conservative numerical solution for the unsaturated flow equation, *Water Resour. Res.*, **26(7)**, 1483–1496, 1990.

[10] H.L. Cloke, J.-P. Renaud, A.J. Claxton, J.J. McDonnell, M.G. Anderson, J.R. Blake and P.D. Bates, The effect of model configuration on modelled hillslope-riparian interactions, *J. of Hydrology*, **279** 167–181, 2003.

[11] R.H. Brooks and A.T. Corey, Hydraulic properties of porous media, *Hydrol. Pap.*, **3**, Colo. State Univ., Fort Collins, pp. 27, 1964.

[12] Y. Mualem, A new model for predicting the hydraulic conductivity of unsaturated porous media. *Water Resour. Res.*, **12**, 513–522, 1976.

[13] M.Th. van Genuchten, A closed-form equation for predicting the hydraulic conductivity of unsaturated soils, *Soil Sci. Soc. Am.*, **44**, 892–898, 1980.

[14] A. Lencastre,*Hydraulique gnrale*, Editions Eyrolles Paris, ISBN, 1999.

[15] R.Moussa and C. Bocquillon, Criteria for the choice of flood routing methods in natural channels, *J. of Hydrology*, No.**186**, 1–30, 1996.

[16] W. Zhang and T. Cundy, Modeling of two-dimensional overland flow, *Water Resour. Res.*, **25(9)**, 2019–2035, 1989.

[17] J.E. VanderKwaak and K. Loague, Hydrologic-response simulations for the R-5 catchment with comprehensive physics-based model, *Water Resour. Res.*, **37(4)**, 999–1013, 2001.

[18] Y.B. Liu, S. Gebremeskel, F. De Smedt, L. Hoffmann and L.Pfister, A diffusive transport approach for flow routing in GIS-based flood modeling, *J. of Hydrology*, No.**283**, 91–106, 2003.